Applications of Polymer, Composite, and Coating Materials

3D Dielectric Layer Enabled Highly Sensitive Capacitive Pressure Sensors for Wearable Electronics

Shufang Zhao, Wenhao Ran, Depeng Wang, Ruiyang Yin, Yongxu Yan, Kai Jiang, Zheng Lou, and Guozhen Shen

ACS Appl. Mater. Interfaces, **Just Accepted Manuscript** • DOI: 10.1021/acsami.0c09893 • Publication Date (Web): 22 Jun 2020

3D Dielectric Layer Enabled Highly Sensitive Capacitive Pressure Sensors for Wearable Electronics

Shufang Zhao,[†] Wenhao Ran,[†] Depeng Wang,[†] Ruiyang Yin,[†] Yongxu Yan,[†] Kai Jiang,[‡] Zheng Lou,[†,□] Guozhen Shen*[†]*

[†] State Key Laboratory for Superlattices and Microstructures, Institute of Semiconductors, Chinese Academy of Sciences & Center of Materials Science and Optoelectronic Engineering, University of Chinese Academy of Sciences, Beijing 100083, China.

[‡] Institute & Hospital of Hepatobiliary Surgery, Key Laboratory of Digital Hepatobiliary Surgery of Chinese PLA, Chinese PLA Medical School, Chinese PLA General Hospital, Beijing 100853, P.R. China

[□] State Key Laboratory of Transducer Technology, Aerospace Information Research Institute, Chinese Academy of Sciences, Beijing, China.

ABSTRACT

Flexible capacitance sensors play a key role in wearable devices, soft robots and the Internet of things (IoT). To realize these feasible applications, subtle pressure detection under various conditions is required and it is often limited by low sensitivity. Herein, we demonstrate a capacitive touch sensor with excellent sensing capabilities enabled by a three-dimensional (3D) network dielectric layer, combining a natural viscoelastic property material of thermoplastic polyurethane (TPU) nanofibers wrapped with electrically conductive materials of Ag nanowires (AgNWs). Taking advantage of the large deformation and the increase of effective permittivity under the action of compression force, the device has the characteristics of high sensitivity, fast response time and low detection limit. The enhanced sensing mechanism about the 3D structures and the conductive filler were discussed in detail. These superior functions enable us to monitor a variety of subtle pressure changes (pulse, airflow and Morse code). By detecting the pressure of fingers, a smart piano glove integrated with 10 circuits of finger joints is made, which realizes the real-time performance of the piano, and provides the possibility for the application of intelligent wearable electronic products such as virtual reality and human-machine interface in the future.

Keywords: Wearable electronics, Flexible sensors, Piano glove, Health monitoring, Human-machine interfaces

INTRODUCTION

To promote close communication between people and equipment, wearable sensor technology can be integrated into human body and perform a variety of functions, including human-computer interface,[1] intelligent robots,[2-4] health monitoring[5-10] and artificial limbs.[11] In the hardware design and fast-growing market of wearable electronics, high-performance state-of-the-art pressure sensors are actively studied.[12-13] Based on the sensing mechanisms, pressure sensors can be divided into piezoresistive sensor,[14-17] piezoelectric sensor,[18-19] capacitance sensor[20] and transistor sensor.[21-22] Although pressure sensors developed very fast in the past years, many challenges still exist in case of flexible electronics applications. For example, some reported flexible resistive pressure sensors consumed large amounts of direct current, and required high operating voltage of about tens of volts to operate field effect transistor-based sensors to achieve high sensitivity. These challenges make the sensors difficult to meet the needs of targeted wearable applications that require low voltage operation and are subject to strict power constraints. As a result, it is still highly desirable to design new structured flexible pressure sensors with the features of high sensitivity, fast response time and low detection limit to meet the request of wearable applications.

Among the four types of pressure sensors, the capacitive sensor has become the research focus recently due to its rapid dynamic response, outstanding temperature insensitivity and low power consumption. Since the capacitive pressure sensor can be classified as the traditional parallel plate capacitor, it usually faces the drawback of low-pressure sensitivity. To enhance the sensitivity, a general way is to introduce

microstructured dielectric layer or electrode to substitute the conventional flat ones.[23-25] As a result, some complex models are proposed including rough interface,[26-27] micropillar arrays, and microscale pyramid.[28] Unfortunately, complicated and time-consuming mold transfer process based on photolithography technology or chemical etching are usually required to manufacture the designed microstructures, which is difficult to fit for large-scale applications. Therefore, developing an optimal method for 3D network dielectric layer fabrication, which simplifies the manufacturing procedures as well as features the sensitivity is urgently needed.

In this work, we demonstrated a high-performance flexible capacitive sensor based on 3D AgNWs@TPU composite as the dielectric layers by using electrospinning techniques. As-fabricated 3D dielectric layer based capacitive sensors exhibited short response and relaxation time (100 ms), high pressure sensitivity (1.21kPa^{-1}), good repeated loading stability (10 000 cycles) and low detection limit (0.9 Pa). As a proof-of-concept, a piano glove with the capacitance sensor as the functional sensing medium was designed and fabricated, where the precise and free control of different notes can be readily realized. This study is an important step towards the realization of advanced wearable electronic technology with high simplicity and high functionality.

RESULTS AND DISCUSSION

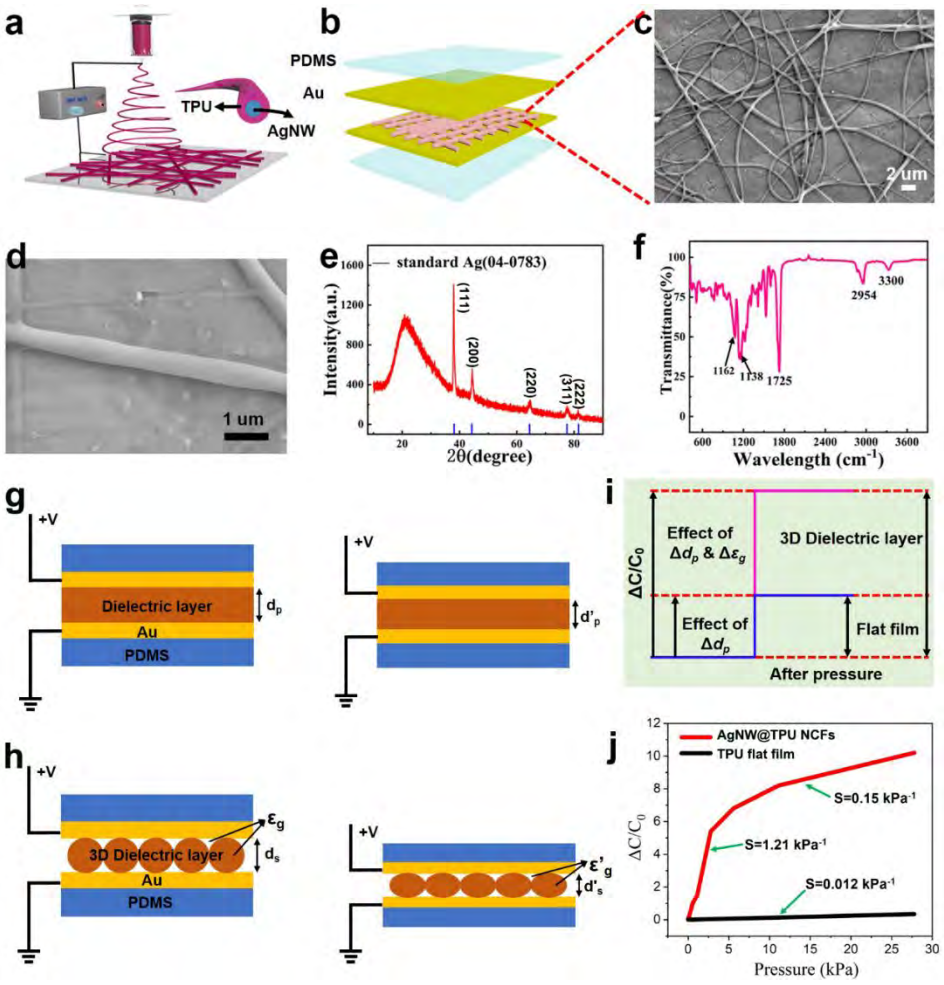

Figure 1. Construction and characterization of flexible capacitance sensors. **(a)** Manufacturing process diagram of the 3D AgNWs@TPU NCFs. **(b)** Schematic illustration of the flexible capacitive sensor with 3D network nanofibers as the dielectric layer. **(c,d)** FESEM image of the AgNWs@TPU nanofibers. **(e)** XRD pattern and **(f)** the FTIR spectra of the composite materials. **(g)** and **(h)** The illustration of the capacitive sensor based on flat dielectric layer and microstructure dielectric layer and its geometry change in the process of loading pressure, respectively. **(i)** The relative change of the interface capacitance of the microstructured film and the flat film under external pressure. **(j)** Pressure sensing capability for different dielectric materials of AgNW@TPU 3D network nanofibers and flat TPU film with a pressure range of up to 28 kPa.

3D AgNWs@TPU network composite films (NCFs) were produced via an efficient, simple electrospinning process, as shown in **Figure 1a**. The detailed process was provided in the experimental section. **Figure 1b** shows the overall structure scheme of the pressure sensor based on the 3D AgNWs@TPU NCFs,

which contains three parts, including AgNWs@TPU, Au and polydimethylsiloxane (PDMS). Briefly, a thin Au film (70 nm) conductive layer was evaporated on PDMS substrate (100 μm) by thermal evaporation method. Subsequently, the Au electrode is covered with a dielectric layer of 3D AgNWs@TPU NCFs. Finally, the fabricated structure is covered on another top gold electrode and assembled into a flexible sandwich capacitive pressure sensor (**Figure S1**).

The morphology and microstructure of the as-synthesized samples obtained via the electrospinning process were characterized using field-emission scanning electron microscope (FESEM) as shown in **Figure 1c**, where composite nanofibers with large length-diameter ratios and the diameters in the range of 500-700 nm can be clearly seen. In **Figure 1d**, a wire-like structure with smooth surface is clearly observed. Moreover, **Figure S2** shows the FESEM images of the as-fabricated AgNWs with an average length of 150 μm and diameter of 100 nm. The successful assembly between the AgNWs@TPU NCFs was also demonstrated by XRD analysis (**Figure 1e**), with a characteristic peak of Ag corresponding to the JPCD No. 04-0783. Moreover, the Fourier transform infrared (FTIR) spectroscopic experiments (**Figure 1f**) also confirm that there is strong attraction between AgNWs and TPU nanofibers.

The pressure sensing mechanisms based on conventional flat and the designed 3D network dielectric layer are schematically illustrated in **Figures 1g-i**, respectively. In

principle, the capacitance (c) of a parallel plate capacitor depends on the distance between the plates (d), the effective area of two electrodes (A) and dielectric constant (ε_r) of the dielectric layer. Due to the high Poisson's ratio of TPU, the A value of the sensor hardly changes when external pressure is applied. Therefore, the capacitance change mainly depends on the change of ε_r and d. Compared with the flat dielectric layer based capacitive sensor, the 3D structure pressure sensor will have larger deformation under the same external pressure. In addition to the reduction of thickness and compression of top and bottom electrodes, the deformation of 3D dielectric layer is much larger than that of flat dielectric layer (**Figure 1g** and **h**). **Figure 1i** shows a graphical interpretation of the relative change in capacitance response to the same pressure applied to the flat film and the 3D structure film. In the case of 3D structure, the deformation of the dielectric layer is more obvious than that of the dielectric layer, which makes the capacitance change much more under the same external pressure. This shows that 3D structure plays a key role in enhancing sensitivity and detecting pressure range. In addition, the increasing effective permittivity caused by the gap contraction between the 3D NCF dielectric layer and the electrode and the changing distance between the TPU nanofibers caused by the deformation under the applied pressure will significantly improve the pressure sensitivity. As a proof of concept, continuous pressure from 0 to 2800 Pa is applied to two sensors in the plane dielectric layer and 3D dielectric layer, respectively. As shown in **Figure 1J**, the sensitivity of the sensor with flat TPU shows typical saturation characteristics (0.012 kPa^{-1}), while the sensor with 3D AgNWs@TPU NCF shows significant sensitivity (1.21 kPa^{-1}). So, compared

with the flat dielectric layer, the sensing performance of the 3D AgNWs NCFs based sensor is significantly improved. Furthermore, the pressure sensitivity of the sensor based on AgNWs@TPU flat film and pure TPU nanofiber networks are also shown in **Figure S3**. These results show that the 3D structure and the introduction of AgNWs on the dielectric layer are the key factors to improve the sensitivity of the pressure sensor.

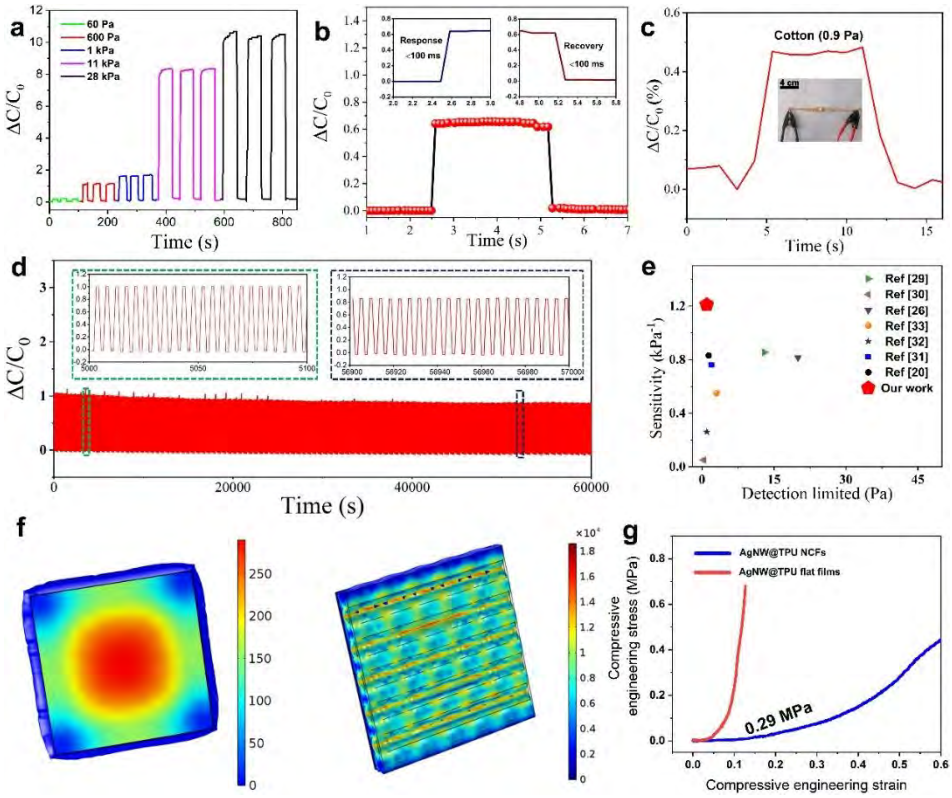

Figure 2 (a) capacitance responses of 3D AgNWs@TPU NCFs based pressure sensor under various applied pressures. **(b)** Transient response and reset time of the device. The inset shows a magnification curve that represents the response time and a reset time of 100 ms. **(c)** Capacitance response of the pressure sensor to the loading and removing of a piece of cotton (≈0.9 Pa). **(d)** The stability of the device response under 10,000 bending cycles. Two insets are magnified cycles of different time periods. **(e)** Sensitivities of our sensor comparison with previous research results. **(f)** FEA of the flat film (left) and 3D structured film (right). **(g)** Compression stress and strain tests on four kinds of TPU materials.

In order to evaluate the repeatability and responsiveness of the designed pressure sensor, the sensing response of the device under various pressures was studied (**Figure 2a**). The result demonstrates that under different loads, the sensor has high sensitivity,

good repeatability, stable capacitive response, and can quickly return to the initial state after pressure relief, indicating that the sensing system has fully released dynamic forces. The response and recovery time of a capacitive sensor applying and releasing pressure was illustrated in **Figure 2b** and its inset. When there is no external pressure, the capacitance of the device hardly changes. However, as the pressure of 2 kPa is applied, the relative capacitance changes from 0 to 0.65 instantaneously, and then remains stable. In contrast, the change in relative capacitance rapidly decreases from 0.65 to 0, when the external pressure is unloaded. Therefore, limited by the accuracy of the test system, the response time of pressure sensor to apply and release pressure is less than 100 ms. These results indicate that our device has a high response stability to static pressure in the process of pressure loading or unloading. For capacitive pressure sensor, the detection ability of ultra-low pressure is also very important. The distinguishable capacitance change in **Figure 2c** is due to the loading and removal of a little cotton, which generates a slight pressure of about 0.9 Pa. The working stability of the flexible pressure sensor is also measured. During 10 000 repeated pressure cycles, the pressure response of each pressure pulse is almost the same, as shown in **Figure 2d**. Moreover, compared with the report shown in **Figure 2e**, our proposed sensor based on a 3D AgNWs@TPU structured dielectric layer has better sensitivity and lower detection limit.[20, 26, 29-33]

To further demonstrate the effect of the 3D microstructure from TPU nanofiber networks, we simulated the stress-strain changes of flat-plate structure and 3D network structures by finite-element analysis (FEA). **Figure 2f** demonstrates the compressive

deformation of a flat structure and a 3D network structure under the same pressure, respectively. For the 3D network structure (the right of **Figure 2f**), a large deformation was observed because the normal force exerted on the upper 3D microstructure film was strongly concentrated on the top of the void feature, rather than the flat film. This confirms that the 3D network is a key design parameter for controlling the air-gap volume, so that the pressure sensor has higher sensitivity. Subsequently, we describe the effect of the corresponding variables on the structure of the dielectric layer at a given pressure (**Figure 2g**). The effective elastic modulus of the 3D AgNWs@TPU NCFs was found to be 0.29 MPa, which is much lower than that of the flat AgNWs@TPU composite film. This is because that compared with flat dielectric layer, the dielectric material of 3D network layer includes air in addition to TPU. Under the same applied pressure, air is more easily compressed than TPU.

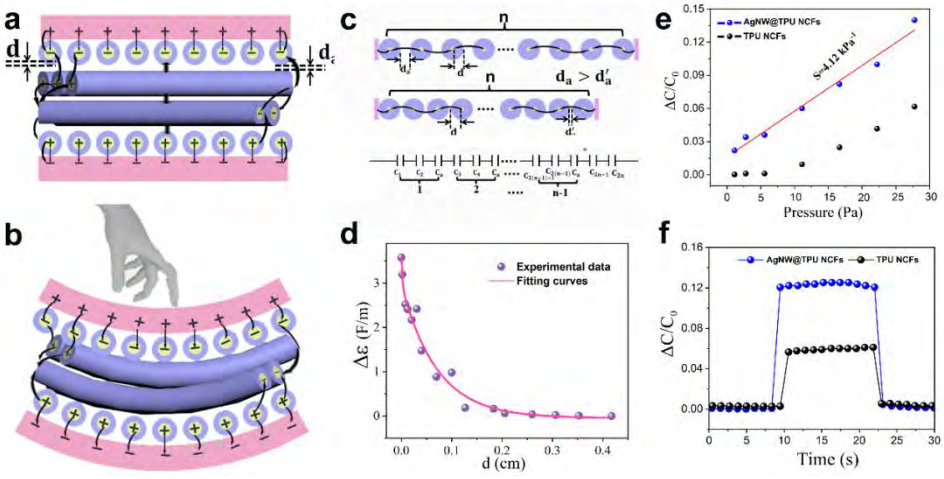

Figure 3 Schematic diagrams of the operating mechanism of the 3D AgNWs@TPU NCFs based capacitive pressure sensor with **(a)** unloading and **(b)** loading stress. **(c)** Detailed view of the 3D AgNWs@TPU NCFs based sensor with and without the stimulus. **(d)** The variation of dielectric constant of sensor with distance. **(e)** Pressure sensing capability for different dielectric materials of 3D AgNWs@TPU NCFs and pure TPU nanofibers under low pressure range up to 30 Pa. (f) Real-time responses to pressure of 30 Pa of the two types of sensors.

In addition to the distance, changes in the dielectric constant also cause changes in the capacitance value. So, by doping different proportion of AgNWs, the dielectric constant can be controlled to enhance the sensitivity of the sensor, as shown in **Figure S4**. The change of the dielectric constant of AgNWs/TPU composite under pressure can be explained by the Kirkpatrick and Zallen statistical percolation model, which is the electrical property of non-interacting random dispersed packing percolation system. Moreover, because the AgNWs are encapsulated in TPU nanofibers, the entire capacitive pressure sensor is equivalent to many small capacitive sensors in series where the AgNWs can be served as the electrodes[34] as shown in **Figure 3a** and upper half of **Figure 3c**. Each small capacitive sensor consists of two AgNWs and dielectric materials, which include air and TPU. The order of dielectric materials is TPU, air, TPU. The dielectric constant of the capacitive pressure sensor can be calculated as:

$$\varepsilon_{eff}=\frac{2nd + (n - 1)d^a}{+}=\frac{(2nd + (n - 1)d^a)\varepsilon\varepsilon^a}{2nd\varepsilon^a + (n - 1)d^a\varepsilon}=\varepsilon-\frac{\varepsilon - \varepsilon^a}{1 + x}, \varepsilon>\varepsilon_a \quad (1)$$

where d is radius of spinning fibers, d_a is distance of single layer air. ε_{eff} is total effective dielectric constant, ε is the dielectric constant of TPU, ε_a is dielectric constant of air. The specific derivation process is shown in Supplement Note1. In **Figure 3b** and second half of **Figure 3c**, when the pressure is applied, the thickness of the TPU dielectric layer does not change and the thickness of the air dielectric decreases. So, the d_a becomes smaller. According to the above function, the ε_{eff} is improved with d_a decreasing. When the pressure is so large that d_a approaches zero, ε_{eff} reaches the maximum. **Figure 3d** shows the relationship between the rate change of the dielectric constant ($\Delta\varepsilon$) and distance in our experiment. Obviously, as the distance increases

meaning the pressure increases, Δε decreases gradually, until it approaches zero. Because Δε is greater than zero, increasing pressure causes ε_{eff} to increase until approaching maximum. Therefore, our theoretical model is consistent with the experimental results. Furthermore, **Figure 3e** and **f** shows the response of the AgNWs@TPU NCF device and the pure TPU nanofibers device under low pressure up to 28 Pa. The results demonstrate that compared with the TPU nanofibers device, the sensitivity of AgNWs@TPU NCF has been significantly improved (4.12 kPa^{-1}), which is consistent with our analysis.

Due to the high response and low detection limit, the device has a reliable choice for real-time detection of human physiological signals. In this work, the pressure sensor based on 3D AgNWs@TPU NCFs is fixed on the wrist with wrist dressing, which can monitor the pulse in real time (**Figure 4a**). **Figure 4b** shows a blood flow pulse recording for more than 6 s, showing a heart rate frequency of approximately 100 beats per minute. Although the capacitance changes little due to the movement of the hand, the sensor can record blood pressure with high sensitivity. **Figure 4c** shows an increase in wrist pulse waveforms with characteristic peak systole (P1) and peak diastole (P2). The radius enlargement index (P2/P1) was 0.74. This value is consistent with the reference value of 25-year-old healthy women in the normal state (170 cm height) in the literature. These data show that our sensors show great potential to continuously monitor daily health with high accuracy and rich medical details. **Figure 4d** shows the photograph of a self-built system for detecting the airflow signals. The curve of relative capacitance with time under the repeated action of three different pressures and gentle

airflow has been shown in **Figure 4e**. With increasing the pressure of the airflow increased, the response of the capacitive pressure sensor increased, which indicate that our capacitive pressure sensor has a good distinguishability for small changes in force. Moreover, our device can also realize the information delivering. As shown in **Figure 4f**, the Morse code is input by touching the surface of the pressure sensor, and the four corresponding characters such as "Semi" are used to indicate the output of the sensing curve of the capacitive response.

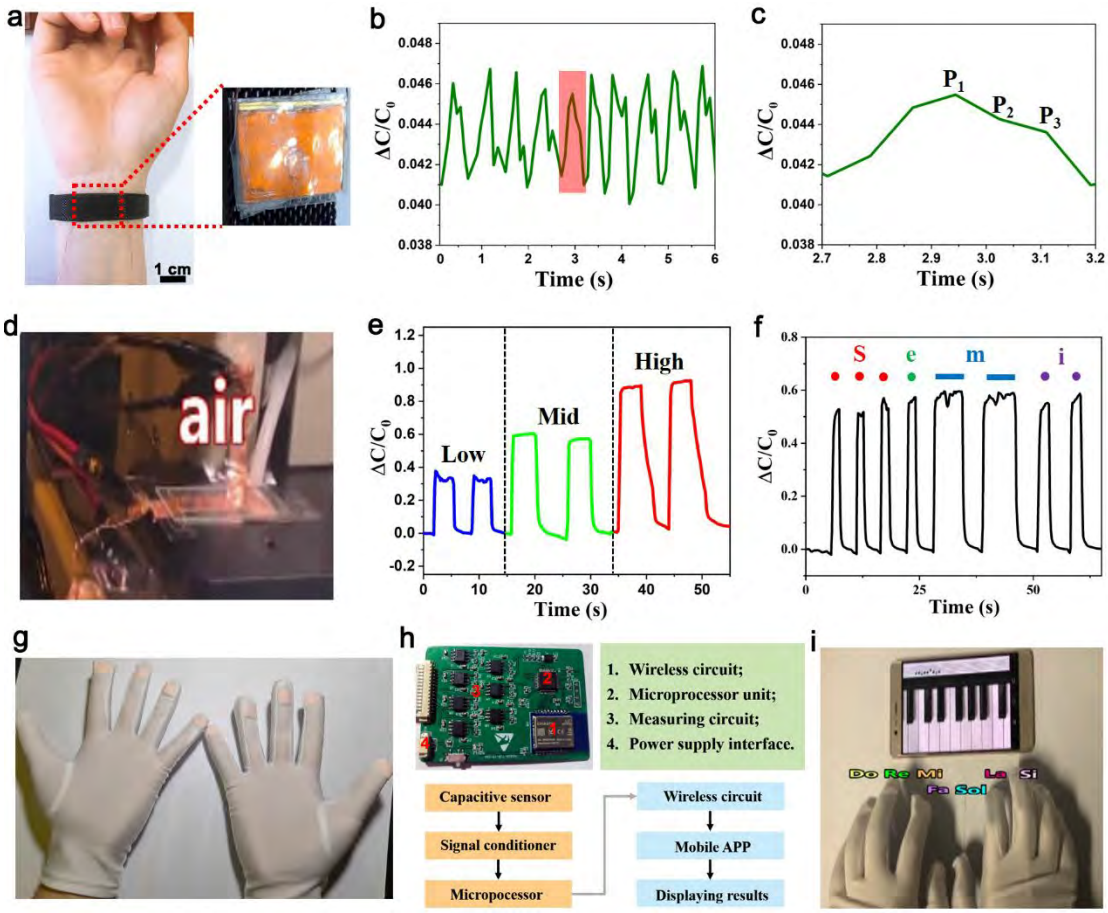

Figure 4 (a) Photograph of a device worn on the wrist to measure blood pressure through a near-surface artery. **(b)** Measurements on the subject's wrist device. **(c)** Single pulse waveform extracted from b. **(d)** The photograph of a self-built system for detecting the air flow signals **(e)** The variation curve of relative capacitance with time under the repeated action of three different pressures of air flow. **(f)** Sensing performance of "Semi" Morse codes produced by touch sensors. **(g)** Photograph of the data glove with ten independent AgNWs/TPU NCF based capacitive sensors. **(h)** Photograph of the printed circuit board (PCB). And the system level

diagram of wireless communication. **(i)** Demonstration of playing the piano based the data glove and displaying in the mobile app.

To realize the practical application of the as-fabricated flexible device in human-computer interaction,[35] we further demonstrate a complex piano glove with ten independent 3D AgNWs@TPU NCFs based capacitive sensors for playing piano. Using a customized ten-channel circuit data acquisition system and real-time analysis software, the test data is received from each capacitive sensor and converted into a digital signal, which is then transmitted to the mobile software. The picture of piano glove is shown in **Figure 4g**, which includes ten basic notes from " do-re-mi-fa-so-la-si " to the higher note " do-re-mi ". Each piano key is a capacitive sensor associated with channels 1 to 10, and its signal can be identified individually. **Figure 4h** exhibits photographs of the logical block diagram and the wireless circuit board of the human-computer interaction system. The capacitive sensor was connected in series with the circuit board. Changes in the pressure can cause changes in the capacitance of the sensor. And then, the processed signal is transmitted to the mobile phone application through the Bluetooth module. Once we touch any button and make effective contact separation action, we can capture the corresponding capacitance change signal and trigger the embedded program at the same time. Movie S1 and **Figure 4i** show a beautiful and smooth melody piano music playback based on a 3D capacitive sensor-based glove piano. Based on this system, a variety of instruments can be realized by simply re-burning the corresponding code into the single-chip microcomputer, which provides a new interactive method for human-machine interface technology.

CONCLUSIONS

In summary, by introducing composite nanofiber-based dielectric layers, we have developed a new type of flexible capacitive pressure sensor with excellent sensor performance. The dielectric layer was successfully prepared by electrospinning the AgNWs@TPU nanofibers mat and the elastic thread are covered around the AgNWs. Compared with traditional capacitive pressure sensor, the 3D composite dielectric layers enhanced sensor possessed a high sensitivity of 1.21 kPa^{-1}, outstanding durability after 10 000 cycles and a rapid response time of 100 ms. The FEA results agree well with the experimental data. It can also be used as a high-performance electronic skin for monitoring various signals from blood pressure pulses to air flow pressure. A 10 channel intelligent piano glove based on capacitance sensor is assembled at each joint of fingertip, which realizes real-time playing of piano. Looking into the future, low-cost methodologies for the preparation of materials and devices will have important value for future applications of wearable electronics in human-machine interface, disease prevention and prosthetic skin devices.

MATERIALS AND METHODS

Synthesis process of AgNWs. 0.2 g Polyvinylpyrrolidone (PVP) was added in 25 mL ethylene glycol and stirred until fully dissolved under 60 ℃. Then, 0.25 g of $AgNO_3$ and 3.5 g of $FeCl_3$ was poured into the above solution with stirring until completely dissolved. The mixed solution was transferred into reaction kettle, immediately and heated at 130 ℃ for 5 h in an oven. And then the precipitate was centrifuged twice at

3500 rpm for 5 min with acetone and ethanol, respectively. Finally, the obtained AgNWs were dispersed in N,N-Dimethylformamide (DMF). The concentration of the solution was 0.3 g/mL.

Synthesis process of AgNWs@TPU nanofibers dielectric layers. First, 4 g Polyurethane (PU) pellets were added in DMF which was held for half an hour and stirred with a magnetic bar for one day until fully dissolved. Then, 4 mL AgNWs solution was poured into the above solution with magnetic stirring for 6 h to obtain the composition solution. Next, we fabricated the AgNWs@TPU nanofibers by electrospinning. The composition solution was added to the syringe and the distance between the syringe needle and aluminum foil (collector) was 25 cm. During spinning, the voltage maintained at 20 kV and the injected speed of the syringe was 1 mL/h with ambient humidity bellowed 40%. One hour later, a thin film of nanofibers was found covered the collector.

Fabrication of the capacitive sensor. First, the PDMS mixture with base and cross-linker at a ratio of 10: 1 was stirred at 30 min. Then, the solution was spin-coated on the Si wafer at 1000 rpm and cured at 80 ℃ for 2 h. Next, a layer of 70 nm Au was deposited on the surface of the cured PDMS. Finally, the PDMS was removed from the Si wafer. According to the method: a layer of gold-plated PDMS, a layer of nanofiber dielectric layer and a layer of gold-plated PDMS, three layers were stacked together to make a pressure sensor. The covered gold surface of the PDMS was contacted with the dielectric layer.

Characterization. The scanning electron microscopy (SEM) was obtained by employing a field-emission SEM (SSX-550, Shimadzu, Japan). A powder XRD (Rigaku D/Max-2550, λ = 1.5418 Å) was used to analyze the crystallinity of AgNWs. The FTIR spectra of the composite materials is characterized by the Nicolet iS10. The static pressure was applied using Instron-E1000. A Keysight 4900a was used to characterize the electrical performance of the capacitive pressure sensor.

ASSOCIATED CONTENT

Supporting Information.

The Supporting Information is available free of charge on the ACS Publications website. Photograph of the flexible sandwich-like capacitor pressure sensor; FESEM images of the AgNWs; pressure sensing capability of dielectric materials and doping different proportions AgNWs; working principle of sensor; real-time piano glove playing (Movie S1).

AUTHOR INFORMATION

Corresponding Author

* E-mail: zlou@semi.ac.cn and gzshen@semi.ac.cn.

Notes

The authors declare no conflict of interest.

ACKNOWLEDGMENT

This work was supported by the National Science Foundation of China (NSFC, Grant No. 61625404, 61874111, 61888102), Young Elite Scientists Sponsorship Program by CAST (2018QNRC001), and China Postdoctoral Science Foundation (2016M601131).

Reference

(1) Liao, X.; Wang, W.; Zhong, L.; Lai, X.; Zheng, Y. Synergistic Sensing of Stratified Structures Enhancing Touch Recognition for Multifunctional Interactive Electronics. *Nano Energy* **2019,** *62*, 410-418.

(2) Zhang, D.; Xu, S.; Zhao, X.; Qian, W.; Bowen, C. R.; Yang, Y. Wireless Monitoring of Small Strains in Intelligent Robots via a Joule Heating Effect in Stretchable Graphene-Polymer Nanocomposites. *Adv. Funct. Mater.* **2020**, 1910809.

(3) Cheng, Y.; Ma, Y.; Li, L.; Zhu, M.; Yue, Y.; Liu, W.; Wang, L.; Jia, S.; Li, C.; Qi, T.; Wang, J.; Gao, Y. Bioinspired Microspines for a High-Performance Spray $Ti_3C_2T_x$ MXene-Based Piezoresistive Sensor. *ACS Nano* **2020,** *14*, 2145-2155.

(4) Liao, X.; Song, W.; Zhang, X.; Zhan, H.; Liu, Y.; Wang, Y.; Zheng, Y. Hetero-contact Microstructure to Program Discerning Tactile Interactions for Virtual Reality. *Nano Energy* **2019,** *60*, 127-136.

(5) Fan, W.; He, Q.; Meng, K.; Tan, X.; Zhou, Z.; Zhang, G.; Yang, J.; Wang, Z. L. Machine-Knitted Washable Sensor Array Textile for Precise Epidermal Physiological Signal Monitoring. *Sci. Adv.* **2020,** *6* (11), eaay2840-eaay2840.

(6) Wang, H.; Song, Y.; Guo, H.; Wan, J.; Miao, L.; Xu, C.; Ren, Z.; Chen, X.; Zhang, H. A Three-Electrode Multi-module Sensor for Accurate Bodily-Kinesthetic Monitoring. *Nano Energy* **2020,** *68*, 104316.

(7) Gao, Y.; Yan, C.; Huang, H.; Yang, T.; Tian, G.; Xiong, D.; Chen, N.; Chu, X.; Zhong, S.; Deng, W.; Fang, Y.; Yang, W. Microchannel-Confined MXene Based Flexible Piezoresistive Multifunctional Micro-Force Sensor. *Adv. Funct. Mater.* **2020**, 1909603.

(8) Tang, X.; Wu, C.; Gan, L.; Zhang, T.; Zhou, T.; Huang, J.; Wang, H.; Xie, C.; Zeng, D. Multilevel Microstructured Flexible Pressure Sensors with Ultrahigh Sensitivity and Ultrawide Pressure Range for Versatile Electronic Skins. *Small* **2019,** *15*, 1804559.

(9) Park, J.; Lee, Y.; Hong, J.; Ha, M.; Jung, Y.-D.; Lim, H.; Kim, S. Y.; Ko, H. Giant Tunneling Piezoresistance of Composite Elastomers with Interlocked Microdome Arrays for Ultrasensitive and Multimodal Electronic Skins. *ACS Nano* **2014,** *8*, 4689-4697.

(10) Liao, X.; Wang, W.; Wang, L.; Tang, K.; Zheng, Y. Controllably Enhancing Stretchability of Highly Sensitive Fiber-Based Strain Sensors for Intelligent Monitoring. *Acs. Appl. Mater. Interfaces* **2019,** *11*, 2431-2440.

(11) Deng, W.; Yang, T.; Jin, L.; Yan, C.; Huang, H.; Chu, X.; Wang, Z.; Xiong, D.; Tian, G.; Gao, Y.; Zhang, H.; Yang, W. Cowpea-structured PVDF/ZnO Nanofibers Based Flexible Self-Powered Piezoelectric Bending Motion Sensor Towards Remote Control of Gestures. *Nano Energy* **2019,** *55*, 516-525.

(12) Wang, X.; Song, W.-Z.; You, M.-H.; Zhang, J.; Yu, M.; Fan, Z.; Ramakrishna, S.; Long, Y.-Z. Bionic Single-Electrode Electronic Skin Unit Based on Piezoelectric Nanogenerator. *ACS Nano* **2018,** *12*, 8588-8596.

(13) Niu, S.; Matsuhisa, N.; Beker, L.; Li, J.; Wang, S.; Wang, J.; Jiang, Y.; Yan, X.; Yun, Y.; Burnetts, W.; Poon, A. S. Y.; Tok, J. B. H.; Chen, X.; Bao, Z. A Wireless Body Area Sensor Network Based on Stretchable Passive Tags. *Nat. Electron.* **2019,** *2*, 361-368.

(14) Wu, P.; Xiao, A.; Zhao, Y.; Chen, F.; Ke, M.; Zhang, Q.; Zhang, J.; Shi, X.; He, X.; Chen, Y. An Implantable and Versatile Piezoresistive Sensor for the Monitoring of Human-Machine Interface Interactions and the Dynamical Process of Nerve Repair. *Nanoscale* **2019,** *11*, 21103-21118.

(15) Sang, Z.; Ke, K.; Manas-Zloczower, I. Design Strategy for Porous Composites Aimed at Pressure Sensor Application. *Small* **2019,** *15*, 1903487.

(16) Wang, K.; Lou, Z.; Wang, L.; Zhao, L.; Zhao, S.; Wang, D.; Han, W.; Jiang, K.; Shen, G. Bioinspired Interlocked Structure-Induced High Deformability for Two-Dimensional Titanium Carbide (MXene)/Natural Microcapsule-Based Flexible Pressure Sensors. *ACS Nano* **2019,** *13*, 9139-9147.

(17) Liao, X.; Liao, Q.; Zhang, Z.; Yan, X.; Liang, Q.; Wang, Q.; Li, M.; Zhang, Y. A Highly Stretchable ZnO@Fiber-Based Multifunctional Nanosensor for Strain/Temperature/UV Detection. *Adv. Funct. Mater.* **2016,** *26*, 3074-3081.

(18) Yan, J.; Han, Y.; Xia, S.; Wang, X.; Zhang, Y.; Yu, J.; Ding, B. Polymer Template Synthesis of Flexible $BaTiO_3$ Crystal Nanofibers. *Adv. Funct. Mater.* **2019,** *29*, 1907919.

(19) Yu, J.; Hou, X.; Cui, M.; Zhang, S.; He, J.; Geng, W.; Mu, J.; Chou, X. Highly Skin-Conformal Wearable Tactile Sensor Based on Piezoelectric-Enhanced Triboelectric Nanogenerator. *Nano Energy* **2019,** *64*, 103923.

(20) Shi, R.; Lou, Z.; Chen, S.; Shen, G. Flexible and Transparent Capacitive Pressure Sensor with Patterned Microstructured Composite Rubber Dielectric for Wearable Touch Keyboard Application. *Sci. China. Mater.* **2018,** *61*, 1587-1595.

(21) Huang, Y.-C.; Liu, Y.; Ma, C.; Cheng, H.-C.; He, Q.; Wu, H.; Wang, C.; Lin, C.-Y.; Huang, Y.; Duan, X. Sensitive Pressure Sensors Based on Conductive Microstructured Air-Gap Gates and Two-Dimensional Semiconductor Transistors. *Nat. Electron.* **2020,** *3*, 59-69.

(22) Park, Y. J.; Sharma, B. K.; Shinde, S. M.; Kim, M.-S.; Jang, B.; Kim, J.-H.; Ahn, J.-H. All MoS2-Based Large Area, Skin-Attachable Active-Matrix Tactile Sensor. *ACS Nano* **2019,** *13*, 3023-3030.

(23) Yao, S.; Zhu, Y. Wearable Multifunctional Sensors Using Printed Stretchable Conductors Made of Silver Nanowires. *Nanoscale* **2014,** *6*, 2345-2352.

(24) Pang, C.; Koo, J. H.; Amanda, N.; Caves, J. M.; Kim, M.-G.; Chortos, A.; Kim, K.; Wang, P. J.; Tok, J. B. H.; Bao, Z. Highly Skin-Conformal Microhairy Sensor for Pulse Signal Amplification. *Adv. Mater.* **2015,** *27*, 634-640.

(25) Lee, J.; Kwon, H.; Seo, J.; Shin, S.; Koo, J. H.; Pang, C.; Son, S.; Kim, J. H.; Jang, Y. H.; Kim, D. E.; Lee, T. Conductive Fiber-Based Ultrasensitive Textile Pressure Sensor for Wearable Electronics. *Adv. Mater.* **2015,** *27*, 2433-2439.

(26) Li, T.; Luo, H.; Qin, L.; Wang, X.; Xiong, Z.; Ding, H.; Gu, Y.; Liu, Z.; Zhang, T. Flexible Capacitive Tactile Sensor Based on Micropatterned Dielectric Layer. *Small* **2016,** *12*, 5042-5048.

(27) Liao, X.; Wang, W.; Lin, M.; Li, M.; Wu, H.; Zheng, Y. Hierarchically Distributed Microstructure Design of Haptic Sensors for Personalized Fingertip Mechanosensational Manipulation. *Mater. Horiz.* **2018,** *5*, 920-931.

(28) Tee, B. C. K.; Chortos, A.; Dunn, R. R.; Schwartz, G.; Eason, E.; Bao, Z. Tunable Flexible Pressure Sensors using Microstructured Elastomer Geometries for Intuitive Electronics. *Adv. Funct. Mater.* **2014,** *24*, 5427-5434.

(29) Tay, R. Y.; Li, H.; Lin, J.; Wang, H.; Lim, J. S. K.; Chen, S.; Leong, W. L.; Tsang, S. H.; Teo, E. H. T. Lightweight, Superelastic Boron Nitride/Polydimethylsiloxane Foam as Air Dielectric Substitute for Multifunctional Capacitive Sensor Applications. *Adv. Funct. Mater.* **2020**, 1909604.

(30) Kim, S. Y.; Park, S.; Park, H. W.; Park, D. H.; Jeong, Y.; Kim, D. H. Highly Sensitive and Multimodal All-Carbon Skin Sensors Capable of Simultaneously Detecting Tactile and Biological Stimuli. *Adv. Mater.* **2015,** *27*, 4178-4185.

(31) Mannsfeld, S. C. B.; Tee, B. C. K.; Stoltenberg, R. M.; Chen, C. V. H. H.; Barman, S.; Muir, B. V. O.; Sokolov, A. N.; Reese, C.; Bao, Z. Highly Sensitive Flexible

Pressure Sensors with Microstructured Rubber Dielectric Layers. *Nat. Mater.* **2010,** *9*, 859-864.

(32) Chen, S.; Zhuo, B.; Guo, X. Large Area One-Step Facile Processing of Microstructured Elastomeric Dielectric Film for High Sensitivity and Durable Sensing over Wide Pressure Range. *Acs. Appl. Mater. Interfaces* **2016,** *8*, 20364-20370.

(33) Boutry, C. M.; Nguyen, A.; Lawal, Q. O.; Chortos, A.; Rondeau-Gagne, S.; Bao, Z. A Sensitive and Biodegradable Pressure Sensor Array for Cardiovascular Monitoring. *Adv. Mater.* **2015,** *27*, 6954-6961.

(34) Wang, M.; Wang, W.; Leow, W. R.; Wan, C.; Chen, G.; Zeng, Y.; Yu, J.; Liu, Y.; Cai, P.; Wang, H.; Ielmini, D.; Chen, X. Enhancing the Matrix Addressing of Flexible Sensory Arrays by a Highly Nonlinear Threshold Switch. *Adv. Mater.* **2018,** *30*, 1802516.

(35) Wang, L.; Lou, Z.; Wang, K.; Zhao, S.; Yu, P.; Wei, W.; Wang, D.; Han, W.; Jiang, K.; Shen, G. Biocompatible and Biodegradable Functional Polysaccharides for Flexible Humidity Sensors. *Research* **2020,** *2020*, 8716847.

Table of Content (TOC)

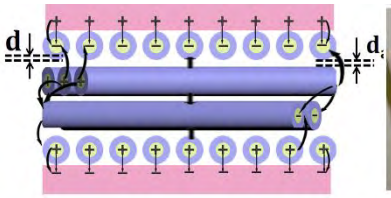
d
d

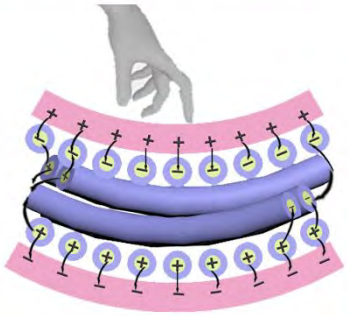


Do Re Mi
La Si
Fa Sol